Frontiers in Environmental Research
Print ISSN: 2960-0251
Online ISSN: 2960-026X
DOI: https://doi.org/10.61784/fer3036

ECOSYSTEM SERVICES SUPPLY–DEMAND DYNAMICS AND MULTIDIMENSIONAL RELATIONSHIPS IN THE SHIYANG RIVER BASIN

ZeTao Chen
Qinghai Institute of Technology, Xining 810000, Qinghai, China.
Corresponding Email: zetaochen@qhit.edu.cn

Abstract: Arid inland river basins are highly sensitive to climate change and anthropogenic disturbances, and persistent imbalances between the supply and demand of ecosystem services have become a critical constraint on regional sustainable development. Taking the Shiyang River Basin, a typical arid inland river basin in northwestern China, as the study area, this research selected four categories of ecosystem services—food provision, water yield, carbon storage, and windbreak and sand fixation. Using a parameter-calibrated InVEST model and GIS-based spatial analysis, we quantified ecosystem services supply and demand from 2000 to 2020, and evaluated supply–demand relationships across three dimensions: quantity matching, spatial matching, and trade-off/synergy assessment. The results show that: (1) From 2000 to 2020, the average supply of food provision and water yield exhibited an increasing trend, whereas carbon storage and windbreak and sand fixation showed fluctuating changes. High food supply was mainly concentrated in oasis areas, while the supply of water yield, carbon storage, and windbreak and sand fixation decreased from the southwest to the northeast; (2) During 2000−2020, the average demand for food provision and carbon storage continued to increase, while the average demand for water yield and windbreak and sand fixation gradually declined. High-demand areas for food provision, water yield, and carbon storage were primarily located in the main urban areas of the oasis, whereas demand for windbreak and sand fixation was mainly distributed in oasis−desert transition zones and desert regions; (3) In terms of quantity matching, food provision and carbon storage were predominantly surplus-oriented, water yield exhibited comparable proportions of surplus and deficit areas, and windbreak and sand fixation were dominated by deficit conditions. For all ecosystem services, low-low spatial matching and synergistic relationships were dominant, with synergy zones accounting for more than 50% of the basin.
Keywords: Ecosystem services; Multidimensional supply–demand relationships; Spatiotemporal differentiation; Shiyang River Basin

1 INTRODUCTION

Global climate change, land degradation, and water scarcity are continuously weakening the functions of ecosystem services (ESs) [1,2]. Northwest China has long faced severe ecological and environmental problems, including vegetation degradation, intensified wind erosion, oasis shrinkage, and excessive exploitation of water resources. Against this background, identifying resource–environment constraints from the perspective of ESs has become an important entry point for ecological management and high-quality development in arid inland river basins.

Research on ES supply–demand relationships in arid basins has primarily focused on evaluating supply patterns, characterizing demand intensity, and identifying supply–demand balance or gaps [3,4]. Although existing studies have made progress in the quantitative characterization of ES supply–demand patterns and spatial heterogeneity, most of them remain at the level of a "static comparison between supply and demand." Comprehensive analyses integrating quantity matching, spatial matching, and trade-off/synergy relationships are still relatively insufficient [4,5].

The SRB, a typical arid inland river basin in northwestern China, is characterized by a distinct "mountain–oasis–desert" gradient, fragile ecological environment, and pronounced conflicts between water-resource supply and demand [6,7]. Under this complex socio-ecological context, focusing solely on ES supply or on a single spatial pattern is insufficient to support refined ecological management at the basin scale. Therefore, it is essential to analyze the supply–demand relationships of multiple ecosystem services in the SRB from the ecological context of the region, and to systematically examine these relationships across the quantity, spatial, and trade-off/synergy dimensions, so as to identify key conflict areas and priority zones for management interventions.

In this study, four major ESs—food production, water yield, carbon storage, and wind−sand fixation—were evaluated using the InVEST model and multi-source spatial datasets. We constructed a comprehensive evaluation framework that integrates supply – demand quantity, spatial matching patterns, and trade-off/synergy relationships. The specific objectives of this research are to: (1) reveal the spatiotemporal evolution of major ES supply−demand patterns in the SRB from 2000 to 2020; and (2) systematically characterize ES supply–demand relationships in terms of quantity matching, spatial distributions, and trade-off/synergy mechanisms, thereby providing scientific evidence for ecological conservation, water-use regulation, and land-use optimization in typical arid inland river basins.

2 MATERIALS AND METHODS

2.1 Study Area Overview

The Shiyang River Basin (SRB) is located in the arid inland region of northwestern China, in the eastern part of the Hexi Corridor, Gansu Province. It is bordered by the Badain Jaran Desert and the Tengger Desert to the north, and by the Qilian Mountains to the south (36°29′N–39°27′N, 101°22′E–104°16′E) (Fig1). The basin covers a total area of 4.16 × 10^4 km² and administratively encompasses three prefecture-level cities (Jinchang, Wuwei, and Zhangye) and seven county-level units (Jinchuan District, Yongchang County, Liangzhou District, Minqin County, Gulang County, and parts of Tianzhu and Subei Counties). The total population is approximately 2.27 million, with an average population density of 55 persons/km².The region experiences a typical temperate continental climate, with a mean annual precipitation of around 200 mm, a mean annual temperature of 7.75 °C, and an annual potential evaporation exceeding 1000 mm. Topographically, the SRB slopes from southwest to northeast, with elevation gradually decreasing from south to north. Three major geomorphological units are distributed from upstream to downstream: mountains, oasis, and desert. The southern mountainous area has a cold semi-humid climate, abundant precipitation, relatively good vegetation cover, and functions as the primary water-yield area. The central oasis zone is dominated by irrigated agriculture and has experienced rapid development; however, intensive water consumption has resulted in severe water scarcity and prominent supply–demand conflicts. The northern desert area is characterized by limited water availability, widespread desertification and soil salinization, and high ecological vulnerability.

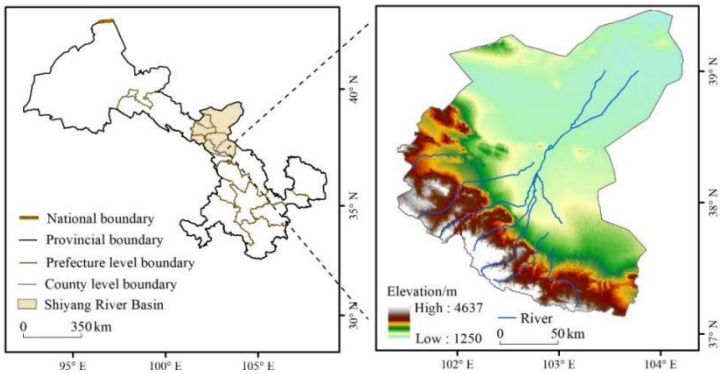

Figure 1 Location of the Study Area
Source: https://www.ngcc.cn

2.2 Data Sources

The data used in this study are listed in Table 1. All datasets were processed with spatial correction, reprojecting, and resampling. A Gauss-Krüger projection was applied, with a central meridian of 102°E, and the spatial resolution was set to 1000m.

Table 1 Data Sources and Descriptions

Data	Source	Resolution
Land Use Data		30m
DEM Data	http://www.resdc.cn	30m
Population Density Data		1km
NDVI	USGS	250m
Precipitation and Evapotranspiration Data	http://www.geodata.cn	1km
Wind Speed and Precipitation Station Data	http://data.cma.cn/	1km
Snow Cover Factor Data	http://www.ncdc.ac.cn/portal/	1km
Soil Data	World Soil Database (HWSD), China Soil Data Set (V1.2)	1km
Socio-Economic Statistical Data	"China Statistical Yearbook," "Gansu Development Yearbook," "Gansu Rural Yearbook," "Gansu Water Resources Bulletin," and various municipal statistical yearbooks	—
Basic Geographical Data	https://www.ngcc.cn	—

2.3 Ecosystem Service Supply and Demand Assessment

2.3.1 Food provision

(1) Supply: Food supply plays a crucial role in sustaining human life and supporting regional sustainable development. Studies have shown a significant linear relationship between crop and livestock yields and the Normalized Difference Vegetation Index (NDVI) [8]. By spatially modeling agricultural and pastoral output using land use data and NDVI, the food supply potential of a region can be more accurately assessed. Specifically, agricultural output is distributed based on the ratio of raster NDVI values to the total NDVI value of cultivated land, pastoral output is allocated using the ratio of raster NDVI values to the total NDVI value of grassland, and aquatic product output is distributed according to the ratio of raster NDVI values to the total NDVI value of water bodies. This method enables a more detailed characterization of food supply capacity at the grid level, thereby quantifying the actual food supply provided in the Shiyang River Basin. The calculation formula is as follows:

$$F_i = F_{sum} \times \frac{NDVI_i}{NDVI_{sum}} \quad (1)$$

In the formula, F_i represents the unit yield of agricultural and pastoral products assigned to grid i; F_{sum} is the total yield of agricultural and pastoral products in the Shiyang River Basin; $NDVI_i$ is the NDVI value for grid$i$; $NDVI_{sum}$ is the sum of the NDVI values of cultivated land, grassland, and water bodies in the Shiyang River Basin.

(2) Demand: The calculation of food demand is based on the per capita food demand standards for Gansu Province published by the National Bureau of Statistics of China. The food demand is estimated by multiplying per capita food demand by population density [9]. The calculation formula is as follows:

$$F_i = F_{per} \times P_{ipop} \quad (2)$$

In the formula, F_i represents the food demand for grid i, F_{per} is the per capita food demand, and P_{ipop} is the population density of grid i.

2.3.2 Water yield

(1) Supply: Water yield supply refers to the ability of ecosystems to regulate the distribution of water resources by intercepting and storing precipitation, which helps mitigate surface runoff, improve regional water cycling, and maintain ecological balance. In the Shiyang River Basin, due to its arid and water-scarce nature, evaluating the supply capacity of water yield supply is crucial for ensuring the sustainable use of regional water resources and the health of ecosystems. Quantifying this service provides scientific support for water resource management, land use planning, and ecological restoration. The InVEST model is the most effective method for quantifying the supply of water yield supply in the Shiyang River Basin [10]. The calculation formula is as follows:

$$W_{xj} = \left(1 - \frac{AET_{xj}}{P_x}\right) \times P_x \quad (3)$$

In the formula, W_{xj} represents the water supply (mm) for grid x of the j land use type, AET_{xj} is the average annual evapotranspiration (mm) for grid x of the j land use type, and P_x is the average annual precipitation (mm) for grid x.

(2) Demand: Water yield demand refers is calculated based on the total water consumption. Water usage for industrial, agricultural, residential, and ecological purposes is distributed across various land use types, including built-up areas, cultivated land, urban land, rural residential areas, forests, and grasslands. This distribution enables the calculation of water yield demand for each grid cell [11].

$$D_Y = D_{agricultural} + D_{industrial} + D_{domestic} + D_{ecological} \quad (4)$$

In the formula, ： D_Y represents the total water yield demand, while $D_{agricultural}$、$D_{industrial}$、$D_{domestic}$、$D_{ecological}$ correspond to agricultural water use, industrial water use, domestic water use, and ecological water use (m^3), respectively.

2.3.3 Carbon storage

(1) Supply: Carbon storage supply refers to the ability of ecosystems to absorb and store carbon, thereby reducing atmospheric carbon dioxide concentrations and mitigating global warming [12]. The InVEST model can accurately estimate the supply for carbon storage. The calculation formula is as follows:

$$S_{cs} = C_{above} + C_{below} + C_{soil} + C_{dead} \quad (5)$$

In the formula, S_{cs} represents the total Carbon storage supply (t/hm²), with C_{above}、C_{below}、C_{soil} and C_{dead} referring to aboveground biomass carbon (t/hm²), belowground biomass carbon (t/hm²), soil organic carbon (t/hm²), and dead organic matter (t/hm²), respectively.

(2) Demand: Based on the carbon emission conversion factor (0.68) published by the Chinese government, the standard coal consumption in the Shiyang River Basin is converted into carbon emissions, which is then divided by the population of the basin to obtain the per capita carbon emissions. Finally, by combining the population density of the Shiyang River Basin, the carbon storage demand in the basin is calculated.

$$D_{cs} = D_{pcfc} \times D_{pop} \quad (6)$$

In the formula, D_{cs} represents the carbon storage demand (t), D_{pcfc} is the per capita carbon emissions (t), and D_{pop} is the raster population density (people/km²).

2.3.4 Windbreak and sand fixation

(1) Supply: The suppression and stabilization of wind and sand by ecosystems is referred to as wind-sand fixation service. By comparing the difference in soil erosion flux between bare land and vegetated areas, the windbreak and sand fixation supply in the Shiyang River region can be quantified. The Revised Wind Erosion Equation (RWEQ) is an effective method for assessing the supply of windbreak and sand fixation in the region [13]. The calculation formula is as follows:

$$F_S = SL_p - SL_r \quad (7)$$

$$SL_p = \frac{2Z}{sp^2} \times Q_p \times e^{-(z/sp)^2} \quad (8)$$

$$Q_p = 109.8 \times (\mathrm{WF} \times \mathrm{EF} \times \mathrm{SCF} \times K') \quad (9)$$

$$sp = 150.71 \times (WF \times EF \times SCF \times K')^{-0.3711} \quad (10)$$

$$SL_r = \frac{2Z}{sr^2} \times Q_r \times e^{-(z/sr)^2} \quad (11)$$

$$Q_r = 109.8 \times (WF \times EF \times SCF \times K' \times C) \quad (12)$$

$$sr = 150.71 \times (WF \times EF \times SCF \times K' \times C)^{-0.3711} \quad (13)$$

In the formula, F_S represents the supply of windbreak and sand fixation (kg/m²), SL_p is the potential wind erosion amount (kg/m²), SL_r is the actual wind erosion amount (kg/m²), Q_p is the maximum sand transport capacity of potential wind force (kg/m), sp is the actual length of key areas (m), Q_r is the maximum sand transport capacity of actual wind force (kg/m), sr is the length of potential key areas (m), Z represents the downwind distance (taken as 50m), WF is the climate factor (kg/m); EF and SCF are the soil erodibility and soil crusting factors, respectively; K′ and C represent surface roughness and vegetation factors.

(2) Demand: Ecosystem service demand refers to the services or products that humans expect or can obtain, without causing negative impacts or harm. Therefore, in this study, the actual wind erosion amount is used as the demand for windbreak and sand fixation. The calculation formula is as follows:

$$F_D = \frac{2Z}{sr^2} \times Q_r \times e^{-(z/sr)^2} \quad (14)$$

In the formula, F_D represents the demand for windbreak and sand fixation (kg/m²), with the other parameters being the same as those used in the equation.

2.4 Multidimensional Analysis of Ecosystem Services Supply-demand Relationships

2.4.1 Quantity matching analysis

In this study, the Ecosystem Service Supply-Demand Ratio (ESDR) is used to compare the actual supply of ecosystem services with human demand, thereby quantitatively analyzing the degree of matching between the two. The ESDR index provides an effective tool for assessing the balance between ecosystem supply capacity and human demand. By calculating the ratio between supply and demand, it is possible to identify regions or services where supply is insufficient or excessive. This method offers a quantitative basis for further developing ecological management measures, optimizing resource allocation, and enhancing regional sustainable development capacity [1]. The specific calculation formula is as follows:

$$ESDR = \frac{ESS - \mathrm{ESD}}{(ESS_{max} + ESD_{max})/2} \quad (15)$$

In the formula, ESDR represents the ecosystem supply-demand ratio, ESS and ESD represent the actual supply and demand of ecosystem services, respectively, while ESS_{max} and ESD_{max} represent the maximum values of ecosystem service supply and demand. ESDR > 0 indicates that the supply of ecosystem services exceeds the demand, defined as a surplus state; ESDR < 0 indicates that the supply is lower than the demand, defined as a deficit state.

2.4.2 Spatial matching analysis

This study employs the four-quadrant model to explore the supply and demand patterns of different ecosystem services, aiming to identify the spatial discrepancies and potential mismatches between supply and demand within a region. The Z-score standardization method is applied to the supply and demand data of ecosystem services, allowing for a comparative analysis of different service types on a unified scale [14]. The standardized supply is placed on the X-axis, and the demand on the Y-axis, creating a two-dimensional coordinate system. Using the four-quadrant model, ecosystem services in the region are categorized into four matching patterns: high-high spatial matching (areas with both high supply and demand), low-low spatial matching (areas with both low supply and demand), low-high spatial mismatching (areas with low supply but high demand), and high-low spatial mismatching (areas with high supply but low demand). This approach not only reveals the spatial distribution of ecosystem services but also provides a basis for optimizing the allocation of services within the region. Spatial visualization further helps to clearly illustrate the supply and demand relationships between different regions and service types, offering data support for ecological protection, resource management, and sustainable development decision-making.

2.4.3 Trade-offs and synergies in ecosystem services supply–demand

We employed the root mean square deviation (RMSD) to quantify the interaction between ecosystem services supply and demand, thereby characterizing their spatial trade-off relationships [15]. The calculation formulas are as follows:

$$ESS_s = (ESS_i - ESS_{min})/(ESS_{max} - ESS_{min}) \quad (16)$$

$$ESD_d = (ESD_d - ESD_{min})/(ESD_{max} - ESD_{min}) \quad (17)$$

$$\mathrm{TF} = \sqrt{(ESS_s - \overline{ESS_s})^2 + (ESD_d - \overline{ESD_d})^2} \quad (18)$$

$$\mathrm{SY} = 1 - \mathrm{TF} \quad (19)$$

where ESS_s denotes the normalized ecosystem services supply, ESS_i is the actual supply value, and ESS_{max} and ESS_{min} represent the maximum and minimum supply values, respectively. $\overline{ESS_s}$ denotes the expected supply value. ESD_d denotes the normalized ecosystem services demand, ESD_i is the actual demand value, and ESD_{max} and ESD_{min}represent the maximum and minimum demand values, respectively. $\overline{ESD_d}$ denotes the expected demand value.

TF represents the degree of trade-off between ecosystem services supply and demand, whereas SY represents the degree of synergy.

3 RESEARCH RESULTS

3.1 Ecosystem Services Supply and Demand Assessment

3.1.1 Spatiotemporal changes in ecosystem services supply

From 2000 to 2020, the supply of different ecosystem services in the study area changed markedly. Among them, food provision exhibited a pronounced increasing trend, water yield showed a slight overall increase, carbon storage fluctuated within a relatively narrow range, windbreak and sand fixation initially decreased and subsequently increased, with rates of change of –8.66% and 19.97%, respectively (Table 2). Spatially, ecosystem services displayed pronounced regional heterogeneity. High-supply zones of food supply were mainly concentrated in the central oasis regions, and the spatial extent of these high-value areas expanded progressively over time, indicating a substantial overall increase in food production across the basin (Fig 2a1–a4). Water yield supply exhibited a general decreasing gradient from southwest to northeast, accompanied by marked local changes. In particular, the southern Qilian Mountains and parts of the oasis showed notable increases and clear spatial clustering of water yield, whereas water supply declined in most desert areas (Fig 2b1–b4). Carbon storage supply followed a similar southwest–northeast decreasing pattern, with substantial changes in some sectors of the basin. Large areas experienced reductions in carbon sequestration, and only scattered small patches showed increases (Fig 2c1–c4). The supply of windbreak and sand fixation exhibited a spatially decreasing trend from southeast to northwest. Significant increases were observed in the Qilian Mountains, oasis zones, and portions of the desert margins, while only limited areas showed decreases, suggesting that wind erosion control measures have produced positive effects (Fig 2d1–d4). Overall, the different ecosystem services presented distinct magnitudes of change and temporal trajectories. The Qilian Mountains and oasis regions functioned as core areas for the enhancement of ecosystem services supply, whereas the desert regions generally maintained low supply levels, with some services still exhibiting declining trends. This pattern indicates a pronounced regional imbalance in the improvement of ecosystem services supply within the basin.

Table 2 Mean Values and Changes in Ecosystem Services Supply–demand from 2000 to 20**20**

Type	Food supply (t/km^2)		Water yield (×10^5 m^3/km^2)		Carbon sequestration (t/hm^2)		windbreak and sand fixation (kg/m^2)	
	Supply	Demand	Supply	Demand	Supply	Demand	Supply	Demand
2000	50.59	18.42	9.22	0.11	2.09	0.03	2.09	28.69
2010	146.7	19.59	9.82	0.09	1.91	0.04	0.9	26.37
2020	196.32	21.87	9.92	0.08	2.29	0.1	2.29	23.50

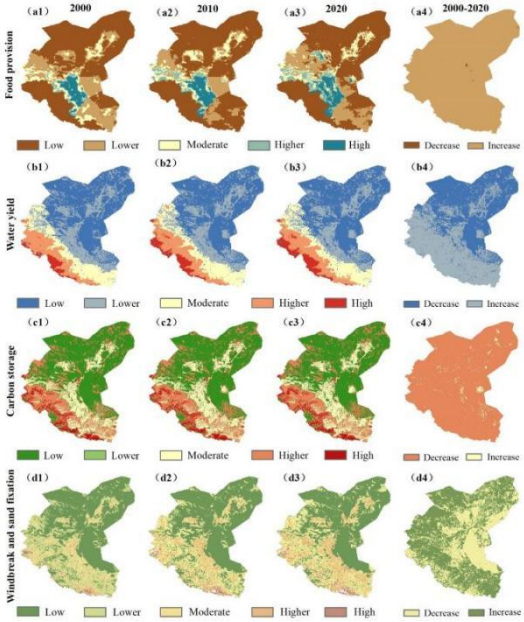

Figure 2 Spatial Distribution and Changes in Ecosystem Services Supply
Source: https://www.ngcc.cn

3.1.2 Spatiotemporal changes in ecosystem services demand

From 2000 to 2020, ecosystem services demand exhibited clear temporal divergence. Average demand increased consistently for food provision and carbon storage, whereas water yield and windbreak and sand fixation showed gradual declines (Table 2). These contrasting trajectories indicate structural shifts in resource use intensity and

environmental regulation needs within the basin. Spatial patterns revealed marked heterogeneity in ecosystem service demand. Food provision demand mirrored the spatial structure of population density and underwent continuous outward expansion, reflecting intensified consumption pressure associated with urban growth and land-use concentration (Fig 3a1–a4). Water yield demand was primarily concentrated in industrial, agricultural, and residential clusters, with high-demand zones expanding mainly within oasis regions and contracting in peripheral areas, suggesting spatial redistribution of water-use pressure (Fig 3b1–b4). Carbon storage demand formed distinct high-value clusters in highly urbanized zones, while remaining low across most other areas; increases were most evident in oasis belts, indicating a growing dependence on local carbon sinks under continued economic expansion (Fig 3c1–c4). In contrast, windbreak and sand fixation demand was concentrated along desert transition zones, with notable increases in eastern Minqin and other desert–gobi sectors, where sparse vegetation and high wind erosion potential maintain persistent regulatory demand (Fig 3d1–d4). Overall, high-demand patterns for food provision, carbon storage, and water yield were tightly associated with population aggregation, industrial activities, and intensive land use within oasis regions, highlighting a strong anthropogenic control on ecosystem service demand. Conversely, windbreak and sand fixation demand was predominantly shaped by biophysical constraints—especially vegetation scarcity, soil exposure, and wind-driven erosion—indicating that ecological vulnerability remains the principal driver in desert–oasis ecotones.

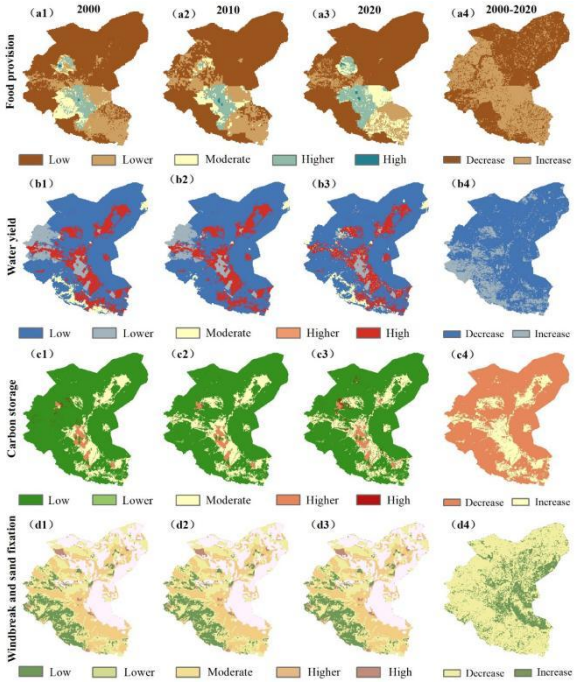

Figure 3 Spatial Distribution and Changes in Ecosystem Services Demand
Source: https://www.ngcc.cn

3.2 Multidimensional Analysis of Ecosystem Services Supply–demand Relationships

3.2.1 Quantity matching analysis

For food provision, surplus conditions overwhelmingly dominated, covering more than 95% of the basin and clustering in oasis regions. Localized deficits within oasis areas progressively transitioned to surplus (Fig. 4a1–a3), suggesting that optimized agricultural input structures and improved water allocation have reduced supply–demand conflicts. This pattern indicates a sustained enhancement of regional food security under continued cropland expansion. The quantity matching of water yield demonstrated a distinct mountain–oasis–desert gradient. Surplus conditions occurred primarily in the Qilian Mountains and adjacent foothill zones, accounting for over 50% of the basin, where high-surplus areas formed a continuous belt along the mountain front. Deficit conditions were concentrated in desert regions (Fig. 4b1–b3). High water yield capacity in the Qilian Mountains reflects extensive forest–grassland cover and favorable runoff generation, whereas oasis regions experience intensified demand derived from concentrated agricultural and residential water use. In desert zones, limited precipitation and fragile ecological conditions constrain supply, resulting in chronic deficits. For carbon storage, surplus conditions dominated across the entire basin, with the Qilian Mountains consistently acting as high-surplus cores (Fig. 4c1–c3). Ecological restoration projects—including widespread afforestation under Grain-for-Green—have enhanced vegetation structure and carbon accumulation. Concurrently, although economic expansion has increased carbon emissions, energy-saving policies and industrial restructuring have moderated emission growth, maintaining a basin-wide surplus in carbon storage. In contrast, windbreak and sand fixation remained dominated by deficit conditions, exceeding 95% of the basin area, with only scattered surplus patches (Fig. 4d1–d3). Persistent deficits reflect low vegetation cover, extensive desert–gobi surfaces, and high wind erosion potential, which maintain strong regulation demand. Nonetheless, long-term ecological engineering—such as shelterbelt

construction, desertification control projects, and high-standard farmland development—has incrementally reduced wind erosion intensity, suggesting gradual mitigation of structural regulatory deficits rather than full supply restoration.

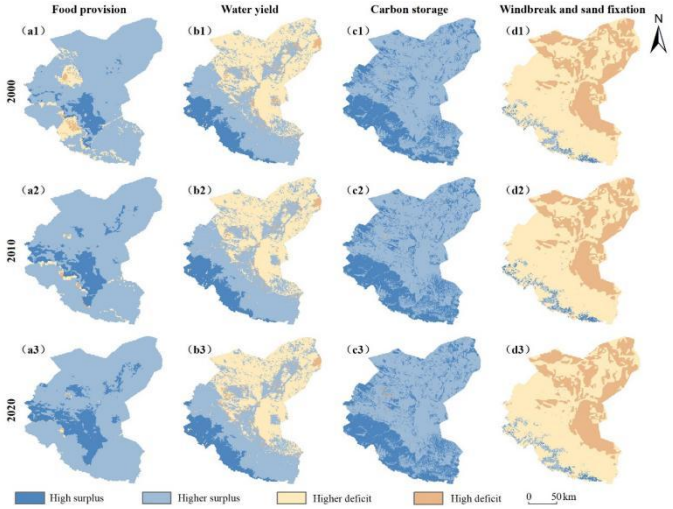

Figure 4 Spatial Distribution of Quantity Matching Relationships in Ecosystem Services Supply–demand
Source: https://www.ngcc.cn

3.2.2 Spatial matching analysis

From 2000 to 2020, spatial matching for food provision was consistently dominated by low–low matching areas (Fig. 5a1–a3). High–high clusters were restricted to oasis cores, whereas high–low mismatches occurred in localized central oasis sectors (e.g., Minqin). Low–high mismatches appeared sporadically in Gulang and Yongchang, comprising a minor share of the basin. The concentration of low–low matching (56%) across the northwestern desert–gobi belt reflects structurally weak agricultural production potential constrained by environmental limitations rather than temporary demand shocks. Spatial matching of water yield exhibited a clear mountain–oasis–desert gradient, with low–low matching (51%) dominating desert regions and high–low mismatching (27%) concentrated along the Qilian Mountain front (Fig. 5b1–b3). High–high matching and low–high mismatching zones were comparatively small and occurred mainly in oasis and transitional foothill areas. This pattern indicates that topographically driven runoff generation in mountain areas is insufficient to offset demand intensification in densely populated oasis belts, generating persistent supply–demand decoupling toward desert margins. For carbon storage, spatial matching was overwhelmingly dominated by low–low and high–low types (95%) distributed across the Qilian Mountains and desert regions (Fig. 5c1–c3). High–high patches were confined to central oasis zones and contracted over time, consistent with vegetation aging effects and limits on additional carbon accumulation under stabilized land use. The rarity of low–high mismatching suggests that carbon demand seldom exceeds supply outside intensive urbanization clusters, reinforcing the role of restoration programs as the primary supply-side control. Spatial matching for windbreak and sand fixation was governed by low–low and high–low patterns (69%), distributed mainly in mountainous and oasis regions (Fig. 5d1–d3). High–high matching occurred only as small, isolated patches, while low–high mismatches (29%) clustered along the Minqin Oasis margin and lower Shiyang River desert transition zones. This configuration indicates that wind erosion regulation remains structurally supply-limited due to sparse vegetation and high aeolian energy, with ecological engineering (e.g., shelterbelts, desertification control, farmland protection) delivering incremental mitigation rather than systemic balancing.

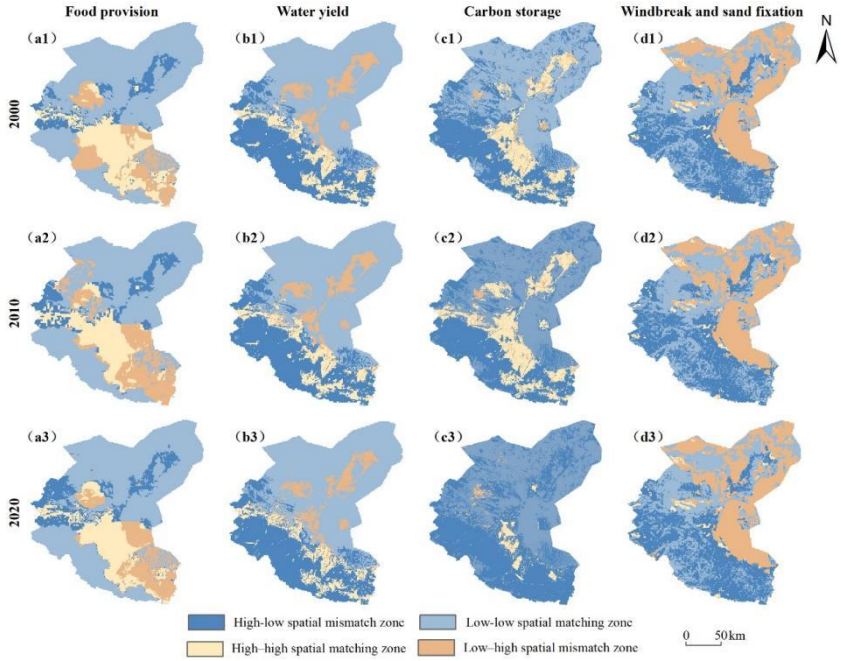

Figure 5 Spatial Distribution of Spatial Matching Relationships in Ecosystem Services Supply–demand
Source: https://www.ngcc.cn

3.2.3 Trade-off and synergy analysis

Spatial patterns of trade-offs and synergies among ecosystem service supply and demand exhibited pronounced geographic differentiation. For food provision, synergy relationships dominated (>70%), primarily distributed across desert sectors and the eastern Qilian Mountains. Notably, the spatial extent of strong synergy progressively contracted over time, indicating a weakening co-benefit structure under intensified agricultural production. Trade-off areas were limited and concentrated in oasis cores (e.g., Minqin and Liangzhou), and remained comparatively stable in spatial extent (Fig. 6a1–a3). For water yield, synergy relationships also prevailed (>70%), with strong synergy concentrated in desert regions and weak synergy forming along mountain–oasis transition belts (Fig. 6b1–b3). Trade-off zones represented a small proportion of the basin and were primarily located in the Qilian Mountains and oasis districts. Over time, strong trade-off areas systematically transitioned toward weak trade-off patterns, reflecting gradual improvements in water-use efficiency and reduced conflict between natural supply and anthropogenic demand. Carbon storage displayed synergy dominance (>60%), concentrated in oasis and desert zones, with weak synergy prevalent in oases and strong synergy in desert regions (Fig. 6c1–c3). Trade-off areas were limited in extent and primarily restricted to the Qilian Mountains, occurring elsewhere only sporadically at small scales. This indicates that ecological restoration and land management policies effectively stabilized carbon supply–demand relations outside high-elevation energy-intensive zones. For windbreak and sand fixation, synergy relationships accounted for ~50%, mainly located in oasis districts and selected desert margins (Fig. 6d1–d3). Trade-off zones were comparatively minor and distributed in the Qilian Mountains and portions of the desert fringe, with weak trade-off dominating mountainous sectors and strong trade-off localized within high aeolian energy environments. Overall, spatial configurations of trade-offs and synergies remained relatively stable with limited temporal variability, demonstrating structural persistence governed by vegetation cover, wind-energy gradients, and long-term ecological engineering interventions.

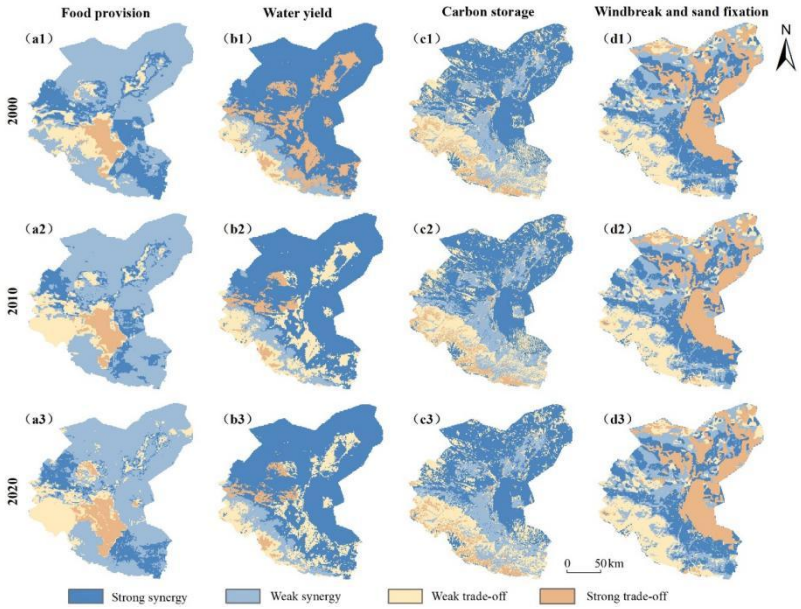

Figure 6 Spatial Distribution of Trade-offs and Synergies in Ecosystem Services Supply–demand Relationships
Source: https://www.ngcc.cn

4 DISCUSSION

This study developed a comprehensive evaluation framework that integrates supply–demand quantity, spatial quadrant matching, and synergy–trade-off analysis, aimed at characterizing ecosystem services supply–demand relationships and their temporal evolution in an arid inland river basin. The framework specifically addresses the dual impacts of natural processes and human activities, and the distinct spatial heterogeneity associated with supply–demand imbalances in such regions. Traditional valuation approaches, such as value-equivalent coefficients and supply–demand evaluation matrices, offer operational simplicity but have limited capacity for spatially explicit identification of supply–demand patterns. These shortcomings are particularly evident in landscape systems with strong geomorphological contrasts between oasis, desert, and mountain environments, where such methods are unable to pinpoint specific imbalance zones or uncover underlying drivers [16-18]. In contrast, the grid-based quantitative assessment adopted in this study directly couples supply capacity with actual demand, enabling identification of overall "surplus supply" or "unmet demand" states from the quantitative dimension. The spatial quadrant model identifies specific hotspots of spatial mismatch and delineates supply–demand discontinuities, while the synergy–trade-off analysis reveals inter-service constraints and potential ecological costs [19]. The results demonstrate that this three-dimensional framework not only identifies concentrated zones of "high supply–low demand," supply–demand discontinuities, and synergy–trade-off hotspots at the basin scale, but also uncovers dominant controlling factors and evolutionary mechanisms, thereby confirming the applicability and explanatory power of quantity–space–synergy integrated analysis in arid inland river basins.

In evaluating ESs in arid inland river basins, the regional adaptability of the modeling approach is often more critical than the choice of the model itself. The default parameter system of the InVEST model was primarily developed for humid or semi-humid regions. Direct application in arid environments typically overestimates vegetation contributions, underestimates wind erosion intensity, and fails to capture the aggregation effects of oasis agriculture [20-22]. Instead of using default settings, this study performed targeted modifications to individual ES modules based on the "mountain recharge–oasis cultivation–desert dissipation" structure of hydrology and vegetation in the Shiyang River Basin. For food production, the combination of "county-level statistics–NDVI weighted spatial allocation" minimized scale-induced bias associated with generalized yield coefficients in oasis agricultural systems. The water yield module incorporated multi-factor constraints including precipitation, evapotranspiration, soil texture, and land use, thereby avoiding the "vegetation increase necessarily enhances water yield" assumption commonly applied in humid regions, and better reflecting the climate threshold-controlled hydrological processes of arid environments. Carbon storage parameters were modified according to precipitation–temperature gradients to prevent systematic overestimation of carbon density in areas with sparse vegetation, aligning with previous findings that carbon sequestration capacity in the Qilian Mountains and the Hexi Corridor is strongly water-limited [19]. For wind–sand fixation, the revised wind erosion mechanism (RWEQ) model explicitly incorporated wind speed, soil particle composition, and surface roughness, thus providing stronger process representation than using NDVI as a single proxy. These adjustments go beyond simple parameter replacements: they significantly enhanced the spatial interpretability of model outputs, with high supply–demand values forming contiguous patterns in oasis regions, stable "supply–demand discontinuities" emerging along mountain recharge zones and desert margins, and temporal trajectories displaying consistent trends of "delayed vegetation recovery followed by progressive enhancement of wind–sand fixation." This evidence indicates that contextual calibration improves the model's ability to capture spatial heterogeneity and process-dominant mechanisms of ESs in arid regions.

This study primarily focused on typical ecosystem services in arid regions and did not explicitly incorporate non-material demands such as landscape aesthetics, cultural recreation, and ecological perception. Consequently, the representation of human well-being structures and the dynamic responses of ecosystem services remains insufficient. Future research could employ emerging perception-based approaches, including public participatory GIS (PPGIS), geo-tagged social media data, and mobile big data, and integrate them with process-based models (e.g., SWAT, RWEQ, and surface evapotranspiration models) to improve the spatial identification of cultural services and enhance the temporal accuracy of ecosystem service assessments in arid regions. Moreover, combining long-term monitoring networks with scenario-based simulations may strengthen the robustness of supply–demand mechanism interpretation and enhance the transferability of cross-basin comparisons.

5 CONCLUSIONS

This study quantified the supply and demand of four ecosystem services using a calibrated InVEST model and GIS–based spatial analysis, and evaluated their multidimensional supply–demand relationships. The main results are as follows:

5.1 Temporal Dynamics of Supply

From 2000 to 2020, the average supply of food provision and water yield increased, whereas the supply of carbon storage and windbreak and sand fixation exhibited marked interannual fluctuations. High supply of food provision was concentrated in the central oasis belt and progressively expanded, while water yield, carbon storage, and windbreak and sand fixation showed a consistent southwest–to–northeast attenuation pattern. These spatial gradients reflect the combined effects of orographic precipitation, land-use intensification in oasis systems, and degraded vegetation structure in desert margins.

5.2 Temporal Dynamics of Demand

Over the same period, demand for food provision and carbon storage continuously rose, whereas demand for water yield and windbreak and sand fixation declined. Spatially, high demand for food provision, water yield, and carbon storage was concentrated in urbanized core areas of the oasis, indicating intensified anthropogenic pressure associated with population aggregation and industrial expansion. In contrast, windbreak and sand fixation demand remained highest in oasis–desert ecotones and desert hinterlands, driven by persistent wind erosion exposure and low vegetation cover.

5.3 Multidimensional Supply–demand Matching

Quantity matching revealed clear divergence among services. Food provision and carbon storage were dominated by surplus conditions (>95% of the basin), water yield exhibited comparable proportions of surplus and deficit zones, and windbreak and sand fixation remained persistently deficit-driven (>95% deficit area). Spatial quadrant analysis indicated that low–low matching types were dominant for all services, particularly in desert basins and oasis fringes, implying structurally low supply–low demand equilibria in environmental resource–limited landscapes. Trade-off/synergy analysis further demonstrated that synergistic interactions prevailed (>50% of the basin), with distinct regional partitioning: synergy dominated in desert matrices, while trade-offs were concentrated in the Qilian Mountain foothills and selected oasis clusters, consistent with competing biophysical controls on water allocation, vegetation recovery, and disturbance regulation.

Overall, the results reveal that ecosystem service enhancement in the Shiyang River Basin remains highly spatially uneven, strongly constrained by topographic gradients, vegetation conditions, and anthropogenic water–energy–land demands, highlighting the necessity of region-specific management rather than uniform basin-wide interventions.

COMPETING INTERESTS

The authors have no relevant financial or non-financial interests to disclose.

REFERENCES

[1] Wei Y, Lu H, Wang J. Dual influence of climate change and anthropogenic activities on the spatiotemporal vegetation dynamics over the Qinghai-Tibetan plateau from 1981 to 2015. Earth's Future, 2022, 10(5): 135-138.

[2] R Costanza, R de Groot, P Sutton, et al. Turner Changes in the global value of ecosystem services Glob. Environ. Chang, 2014, 26, 152-158.

[3] Zhai T, Zhang D, Zhao C. How to optimize ecological compensation to alleviate environmental injustice in different cities in the Yellow River Basin? A case of integrating ecosystem service supply, demand and flow. Sustainable Cities and Society, 2021, 75, 101-106.

[4] Teng Y, Chen G, Su M. Ecological management zoning based on static and dynamic matching characteristics of ecosystem services supply and demand in the Guangdong–Hong Kong–Macao Greater Bay Area. Journal of Cleaner Production, 2024, 448, 141-145.
[5] Zhao Q, Chen Y, Cuan Y. Application of ecosystem service bundles and tour experience in land use management: A case study of Xiaohuangshan Mountain (China). Remote Sensing, 2021, 13(2): 242-243.
[6] Men D, Pan J. Integrating key species distribution and ecosystem service flows to build directed ecological network: Evidence from the Shiyang River Basin, China. Journal of Environmental Management, 2025, 381, 125-127.
[7] Wang Y, Pan J. Landscape-based ecological resilience and impact evaluation in arid inland river basin: A case study of Shiyang River Basin. Applied Geography, 2024, 167, 103-109.
[8] Chen T, Feng Z, Zhao H, et al. Identification of ecosystem service bundles and driving factors in Beijing and its surrounding areas. Science of the Total Environment, 2020, 711, 101-106.
[9] Tang H J, Li Z M. Study on per capita grain demand based on Chinese reasonable dietary pattern. Scientia Agricultura Sinica. 2012, 45(11): 2315-2327.
[10] Wang H, Wang L, Fu X, et al. Spatial-temporal pattern of ecosystem service supply-demand and coordination in the Ulansuhai Basin, China. Ecological Indicators. 2022, 143, 109-112.
[11] Chen J, Jiang B, Bai Y, et al. Quantifying ecosystem services supply and demand shortfalls and mismatches for management optimisation. Science of the Total Environment. 2019, 650, 143-149.
[12] Liu L, Wu J. Ecosystem services-human wellbeing relationships vary with spatial scales and indicators: The case of China. Resources, Conservation and Recycling. 2021, 172, 105-112.
[13] Gong J, Shi J, Zhu C, et al. Accounting for land use in an analysis of the spatial and temporal characteristics of ecosystem services supply and demand in a desert steppe of Inner Mongolia, China. Ecological Indicators. 2022, 144, 109-116.
[14] Yin D, Yu H, Shi Y, et al. Matching supply and demand for ecosystem services in the Yellow River Basin, China: A perspective of the water-energy-food nexus. Journal of Cleaner Production. 2023, 384, 135-142.
[15] Bradford J B, D'Amato A W. Recognizing trade-offs in multi-objective land management. Frontiers in Ecology and the Environment, 2012, 10(4): 210-216.
[16] Wei W, Nan S, Xie B, et al. The spatial-temporal changes of supply-demand of ecosystem services and ecological compensation: A case study of Hexi Corridor, Northwest China. Ecological Engineering. 2023, 187, 106-112.
[17] Zhou L, Zhang H, Bi G, et al. Multiscale perspective research on the evolution characteristics of the ecosystem services supply-demand relationship in the chongqing section of the three gorges reservoir area. Ecological Indicators. 2022, 142, 109-227.
[18] Sitch S, Smith B, Prentice I C, et al. Evaluation of ecosystem dynamics, plant geography and terrestrial carbon cycling in the LPJ dynamic global vegetation model. Global change biology. 2003, 9(2): 161-185.
[19] Zhang X, Li X, Wang Z, et al. A study on matching supply and demand of ecosystem services in the Hexi region of China based on multi-source data. Scientific Reports, 2024, 14(1): 13-32.
[20] González-García A, Palomo I, González J A, et al. Quantifying spatial supply-demand mismatches in ecosystem services provides insights for land-use planning. Land use policy. 2020, 94, 104-109.
[21] Cui F, Tang H, Zhang Q, et al. Integrating ecosystem services supply and demand into optimized management at different scales: A case study in Hulunbuir, China. Ecosystem Services. 2019, 39, 100-112.
[22] Wang H, Wang L, Fu X. Spatial-temporal pattern of ecosystem service supply-demand and coordination in the Ulansuhai Basin, China. Ecological Indicators, 2022, 143, 109-121.